

## Imaging resonant micro-cantilever movement with ultrafast scanning electron microscopy

Garming, Mathijs W.H.; Kruit, Pieter; Hoogenboom, Jacob P.

**DOI**

[10.1063/5.0089086](https://doi.org/10.1063/5.0089086)

**Publication date**

2022

**Document Version**

Final published version

**Published in**

Review of Scientific Instruments

**Citation (APA)**

Garming, M. W. H., Kruit, P., & Hoogenboom, J. P. (2022). Imaging resonant micro-cantilever movement with ultrafast scanning electron microscopy. *Review of Scientific Instruments*, 93(9), Article 093702. <https://doi.org/10.1063/5.0089086>

**Important note**

To cite this publication, please use the final published version (if applicable). Please check the document version above.

**Copyright**

Other than for strictly personal use, it is not permitted to download, forward or distribute the text or part of it, without the consent of the author(s) and/or copyright holder(s), unless the work is under an open content license such as Creative Commons.

**Takedown policy**

Please contact us and provide details if you believe this document breaches copyrights. We will remove access to the work immediately and investigate your claim.

# Imaging resonant micro-cantilever movement with ultrafast scanning electron microscopy

Cite as: Rev. Sci. Instrum. **93**, 093702 (2022); <https://doi.org/10.1063/5.0089086>

Submitted: 22 February 2022 • Accepted: 11 August 2022 • Published Online: 14 September 2022

 Mathijs W. H. Garming, Pieter Kruit and  Jacob P. Hoogenboom



View Online



Export Citation



CrossMark

## ARTICLES YOU MAY BE INTERESTED IN

[Development of a scanning tunneling microscope for variable temperature electron spin resonance](#)

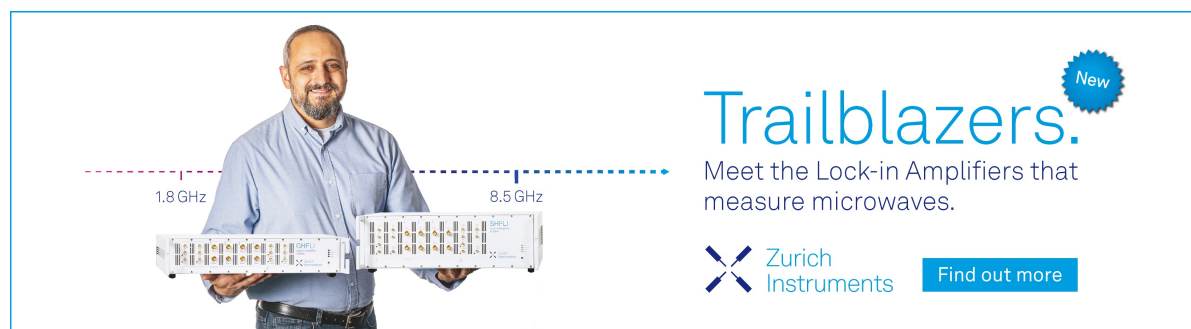
Review of Scientific Instruments **93**, 093703 (2022); <https://doi.org/10.1063/5.0096081>


[Absolute beam monitor: A novel laboratory device for neutral beam calibration](#)

Review of Scientific Instruments **93**, 093302 (2022); <https://doi.org/10.1063/5.0092065>


[Ultrafast scanning electron microscopy with sub-micrometer optical pump resolution](#)

Applied Physics Reviews **9**, 021418 (2022); <https://doi.org/10.1063/5.0085597>



**Trailblazers.** 

Meet the Lock-in Amplifiers that measure microwaves.

 Zurich Instruments [Find out more](#)

# Imaging resonant micro-cantilever movement with ultrafast scanning electron microscopy

Cite as: Rev. Sci. Instrum. 93, 093702 (2022); doi: 10.1063/5.0089086

Submitted: 22 February 2022 • Accepted: 11 August 2022 •

Published Online: 14 September 2022



View Online



Export Citation



CrossMark

Mathijs W. H. Garming,  Pieter Kruit, and Jacob P. Hoogenboom<sup>a)</sup> 

## AFFILIATIONS

Department of Imaging Physics, Delft University of Technology, Delft, The Netherlands

<sup>a)</sup> Author to whom correspondence should be addressed: [j.p.hoogenboom@tudelft.nl](mailto:j.p.hoogenboom@tudelft.nl)

## ABSTRACT

Here, we demonstrate ultrafast scanning electron microscopy (SEM) for making ultrafast movies of mechanical oscillators at resonance with nanoscale spatiotemporal resolution. Locking the laser excitation pulse sequence to the electron probe pulses allows for video framerates over 50 MHz, well above the detector bandwidth, while maintaining the electron beam resolution and depth of focus. The pulsed laser excitation is tuned to the oscillator resonance with a pulse frequency modulation scheme. We use an atomic force microscope cantilever as a model resonator, for which we show ultrafast real-space imaging of the first and even the 2 MHz second harmonic oscillation as well as verification of power and frequency response via the ultrafast movies series. We detect oscillation amplitudes as small as 20 nm and as large as 9  $\mu\text{m}$ . Our implementation of ultrafast SEM for visualizing nanoscale oscillatory dynamics adds temporal resolution to the domain of SEM, providing new avenues for the characterization and development of devices based on micro- and nanoscale resonant motion.

© 2022 Author(s). All article content, except where otherwise noted, is licensed under a Creative Commons Attribution (CC BY) license (<http://creativecommons.org/licenses/by/4.0/>). <https://doi.org/10.1063/5.0089086>

Scanning electron microscopy (SEM) is characterized by resolutions capable of imaging deep below the optical diffraction limit and is, therefore, a fundamental tool for the inspection of nanoscale devices. SEM images have a highly desirable combination of resolution, depth of focus, and ease of interpretation of the data.<sup>1</sup> However, limited time resolution of SEM constrains their applicability to (quasi-)static samples. Long image scanning times of tenths of seconds at least, limited detector bandwidth, and low current in the electron beam are the factors limiting time resolution in conventional SEM.<sup>2</sup> The scan time limitation has been addressed with hyperspectral motion visualization SEM, which analyzes frequency components in the secondary electron signal to gain information on the movement of the sample,<sup>3</sup> but temporal resolution is still limited by detector bandwidth.<sup>2</sup> Ultrafast scanning electron microscopy (USEM), in which a sample is pumped and probed with ultrafast laser and electron pulses, respectively, in a stroboscopic fashion, has been developed to do SEM with time resolutions limited by laser and electron pulse duration.<sup>4</sup>

USEM applications have focused on studying photoexcited charge carrier dynamics in semiconductors, measuring ultrafast lifetimes and diffusion of carriers in a multitude of materials.<sup>5–7</sup> Direct quantitative observation of the motion of micro- and nanoscale objects such as mechanical resonators has to our knowledge not yet

been pursued despite their importance for sensing<sup>8–15</sup> and probe-based microscopy<sup>16,17</sup> and the fact that SEM is routinely used for (static) quality inspection after fabrication. Optical interferometry is typically used to characterize micro- and nanomechanical resonators, but it has limited lateral resolution and the data acquired require extensive analysis and interpretation.<sup>18,19</sup> Ultrafast transmission electron microscopy (UTEM) has been used to measure nonresonant cantilever motion,<sup>20</sup> and the movement of a resonant beam structure has been studied through the analysis of motion blur in images recorded with continuous beam transmission electron microscopy.<sup>21</sup> Further applications of UTEM have focused on measuring strain wave dynamics in thin materials.<sup>22,23</sup> Combining the advantages of SEM with the temporal resolution required for dynamical imaging of high-frequency miniature resonators would enable direct real-space imaging and monitoring amplitude, phase, and frequency under resonant and nonresonant excitation.

Here, we present ultrafast movies of a single clamped beam resonator, an atomic force microscope (AFM) cantilever, performing real-space imaging of the fundamental resonance to demonstrate our approach. We determine the power dependency of the oscillation amplitude and run a frequency sweep to determine the resonator quality factor (Q-factor). Additionally, we capture the 2 MHz

second harmonic oscillation, where USEM enables straightforward visualization of the mode shape while pushing the framerate to an effective 50 MHz.

Our USEM setup [Fig. 1(a)] is based on a commercial scanning electron microscope,<sup>6</sup> which has been modified to enable pulsed beam operation through electron beam blanking<sup>24</sup> and to accommodate femtosecond laser excitation of the sample through an optical objective positioned below the sample in the vacuum chamber. The laser, a Coherent Vitara-T with 800 nm central wavelength and 95 MHz pulse repetition rate, is used in conjunction with a pulse picker based on a Conoptics Model 350-160 E-O Modulator. The pulse picker allows us to control the pulse repetition time and tune the laser excitation rate to the resonator we examine. For these experiments, we have used a NANOSENSORS PPP-NCHR 300 kHz AFM probe, for its trapezoidal cross section and aluminum coating on the detector side make it very suitable for photothermal excitation.<sup>25,26</sup> In this process, laser pulses prompt local heating of the material and thermal expansion initiates a bending motion. The cantilever is mounted horizontally, rotated along the longitudinal axis such that the direction in which the tip points makes a 55° angle with the electron beam [see Fig. 1(a) inset]. This makes the displacement of the cantilever clearly visible in electron beam imaging.

The laser is focused on the back (detector) side of the cantilever [see Fig. 1(a) inset] through a Nikon objective with 10× magnification and an NA of 0.3. Through optical imaging of the laser spot on the sample, we focus the laser near the cantilever base to excite the first mode. A pulse frequency modulation (PFM) scheme is

implemented to approximate sinusoidal excitation near the 300 kHz specified cantilever resonance frequency, which is much lower than the 95 MHz laser pulse repetition frequency. To this end, we operate the laser pulse picker in gated mode, and supply a 1024-character PFM sequence [Fig. 1(b)] to the gating input with a Thurlby Thandar Instruments TG1010A programmable function generator. Laser pulses are only transmitted when the gating input is high, and the PFM sequence is repeated to create periodic modulation. Continuous beam electron imaging easily identifies the resulting movement of the cantilever through motion blur [Fig. 1(c)]. When laser excites the cantilever at its resonance frequency of 316.71 kHz with 48 mW of laser power, we see a multi-micron displacement of the tip. The mode shape features a single node and antinode at the base and tip, respectively, indicating this is the fundamental frequency.

Electron pulses are generated by electron beam blanking, a scheme in which the electron beam travels between two blanker plates with an electric field between them that can deflect the beam over an aperture placed lower in the column. By rapidly switching the polarity of the blanker voltage and thereby the field direction, the beam is quickly swept over the aperture, creating a sub-ns electron pulse during the brief moment the electron beam is directed through the aperture. Electron pulse generation is also triggered by the function generator, synchronizing the laser excitation and electron probing of the cantilever. Pulses as short as 90 ps have been demonstrated on our setup.<sup>24</sup> Longer pulses can be generated by switching the blanker voltage to zero to transmit the beam for as long as the desired pulse duration and then back to the original value

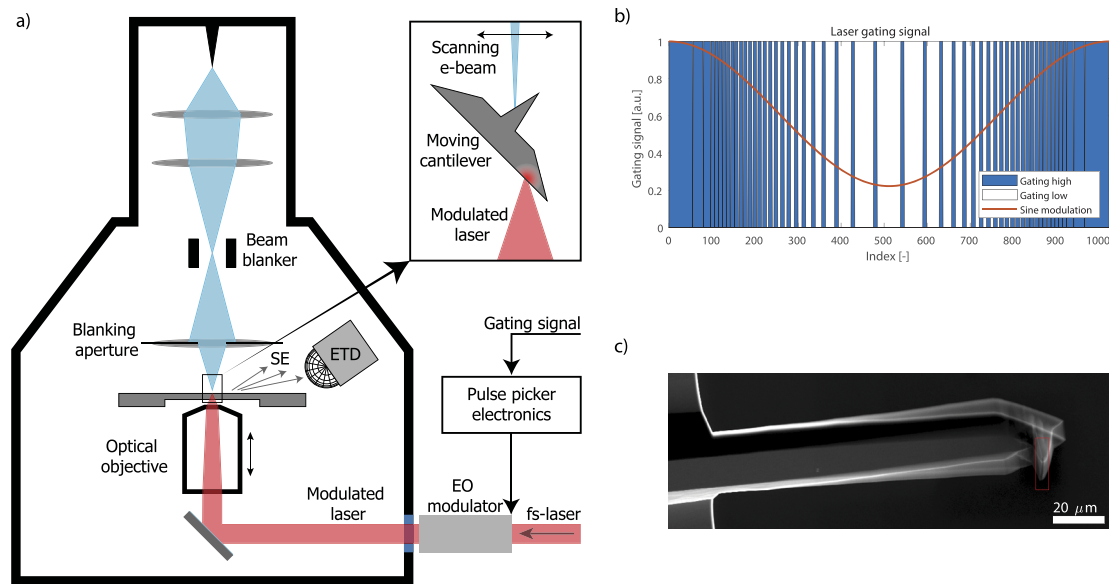


**FIG. 1.** (a) Schematic for USEM on laser-excited resonant cantilevers. Electron pulses, illuminating the sample from above, are created using a beam blanker. The cantilever is excited using a fs-laser focused on the sample via an objective lens below the sample. Secondary electrons (SEs) are used as signal and are detected with an Everhart-Thornley detector (ETD). (b) The fs-laser excitation is modulated with a pulse frequency modulation (PFM) scheme, approximating sinusoidal excitation. We use the pulse sequence to gate the pump laser, resulting in periodic modulation of the laser power to get the cantilever into resonant motion. (c) SEM image of the cantilever recorded with a continuous electron beam with laser actuated near the cantilever base at its 316.71 kHz resonance frequency. A multi-micron amplitude motion is seen through motion blur, with the shape representing the fundamental mode. A detailed view of the region marked by the red box is found in Fig. 2.

to block the beam again. This flexibility in pulse duration offered by beam blanking can be useful as the current in the pulsed beam and consequently the acquired signal is directly proportional to the pulse duration, meaning that longer pulses can drastically shorten measurement times. We, therefore, adapt the pulse duration to the timescale of the dynamics measured, using either 20 ns or 100 ns pulse durations.

Ultrafast movies are constructed from stroboscopic images, recorded by scanning full images of the cantilever with a 10 kV pulsed electron beam and the modulated laser focused on the cantilever [Fig. 2(a)]. As the laser excitation and electron beam probing are phase locked, the cantilever appears to be standing still and the resulting image looks like a regular SE micrograph. Upon completion of an image frame, a phase shift is added to the PFM signal in order to vary the point in the oscillation probed by the electron pulse. The next frame is scanned, showing the cantilever at another point in its oscillatory cycle [Fig. 2(b)], and this is repeated until the phase shifts cover the full  $2\pi$  oscillation. All frames are combined into a video of the oscillatory movement, which constitutes our ultrafast movie.

Stroboscopic imaging with a 20 ns pulsed electron beam allows for time resolved real-space imaging of the beam without significant motion blur. By sequentially acquiring frames and increasing the pump–probe delay in 88 ns steps between scans, we map the full oscillation period and combine the frames into an ultrafast movie of the beam vibration (see Fig. 2, multimedia view). Stroboscopic images recorded with two different delays between cantilever excitation and electron pulse generation are shown in Figs. 2(a) and 2(b), where the cantilever is probed at different time points in the oscillation. Figure 2(c) shows sections of all recorded frames, with the image cropped to the AFM sensing tip for clarity. Difference images between frame zero, which functions as a reference, and the other movie frames can be seen in Fig. 2(d). The tip moves away from its original position until maximum displacement is reached, at which point the tip returns to its starting point with good focus throughout the image sequence. Imaging with 100 ns electron pulses gives more motion blur, but it is an option to reduce noise (see the [supplementary material](#)). Tip displacement relative to the reference frame is quantified using an image shift algorithm<sup>27</sup> [see Fig. 2(e)]. A sinusoidal fit

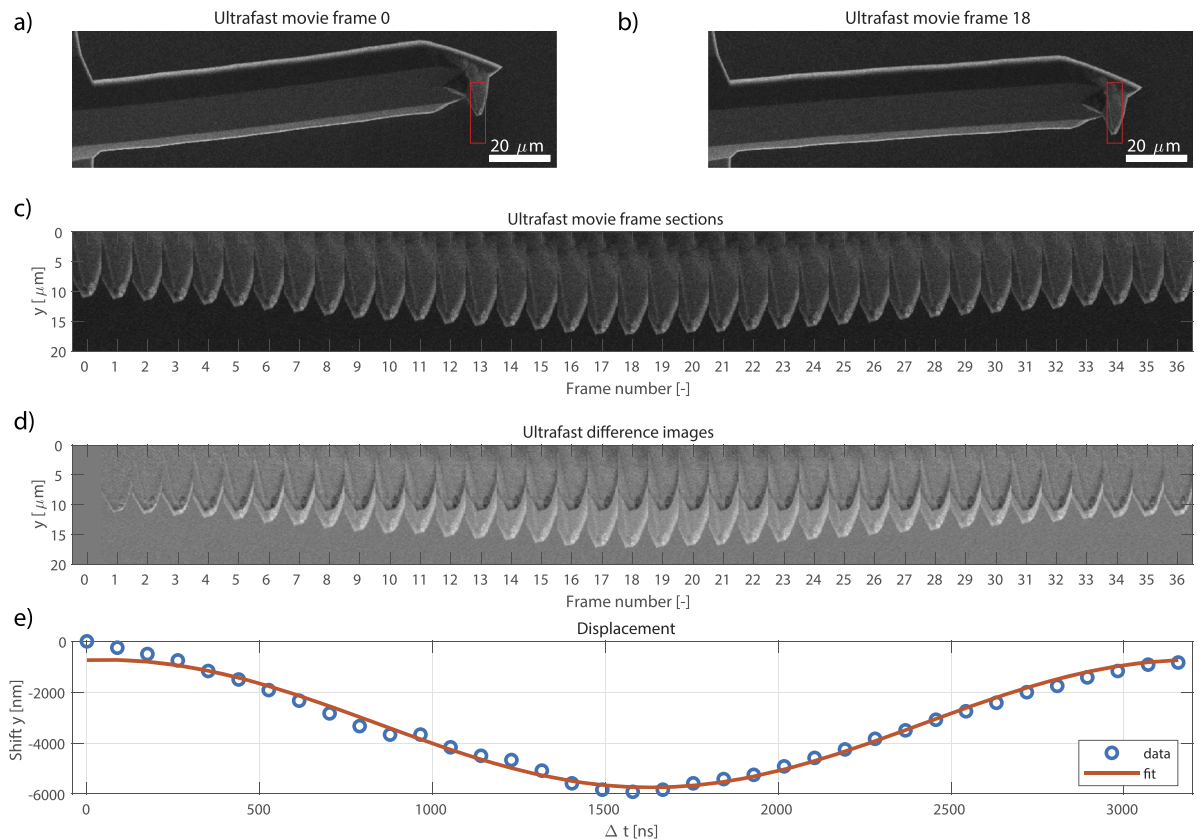


**FIG. 2.** (a) Stroboscopic USEM images of an AFM cantilever are recorded with a pulsed electron beam locked to the laser frequency. The cantilever is excited with the laser and probed with electron pulses at 316.72 kHz. (b) By changing the phase delay [here 1585 ns with respect to (a)] between the cantilever laser excitation and electron pulse generation, stroboscopic images at different time points in the oscillation are recorded. (c) Multiple stroboscopic images are combined into an ultrafast movie of the motion of an AFM cantilever. Shown are sections of the movie frames cropped to the AFM sensing tip, marked by the red box in Figs. 2(a) and 2(b). Each frame corresponds to a 88 ns step. (d) Difference images relative to a reference frame (frame 0, shown in (a)) show the position of the cantilever tip at various times during an oscillation cycle. (e) The tip displacement as a function of laser–electron pulse delay follows a sine curve with an amplitude of  $5.0 \pm 0.2 \mu\text{m}$ . Multimedia view: <https://doi.org/10.1063/5.0089086.1>

represents the data well and indicates a peak–peak amplitude of  $5.0 \pm 0.2 \mu\text{m}$ .

Power dependence of the oscillator amplitude is measured by successively recording ultrafast movies of the cantilever motion at various power levels ranging from 0 to 58 mW. We extract the displacement of the tip from the movie frames [Fig. 3(a)] and fit sinusoidal functions to obtain amplitude data. Figure 3(b) shows the amplitude as a function of laser power, with error bars indicating the fitting uncertainty. Amplitudes are lower than seen in Fig. 2, as we excited slightly off-resonance at 317 kHz to mitigate the effect of frequency drift between acquisition of different movies. We see a consistent trend of increasing amplitude with increasing laser power within the error margins. For low power, the relation is linear, but a saturation effect is observed at high power as illustrated by linear and exponential fits, respectively. The linear fit includes the power levels up to 5.4 mW and yields  $36 \pm 5 \text{ nm/mW}$  at this excitation frequency. Saturation at higher powers is attributed to nonlinear dynamics of the cantilever itself that

become non-negligible at high amplitudes.<sup>28,29</sup> Cantilever amplitude strongly depends on laser focus and spot position as well as the excitation frequency and cantilever type.<sup>26,30</sup> Keeping in mind these possible variations, the measured linear relation at low power and the obtained slope are in line with those found in literature,<sup>31,32</sup> indicating that USEM can be a tool for investigating cantilever power response.

We next characterize the frequency response and Q-factor of the resonator by means of movies recorded with varying the excitation frequency at 42 mW laser power. Figures 3(c) and 3(d) show the amplitude and relative phase of the recorded oscillation as a function of excitation frequency. The resonance frequency at 316.76 kHz is easily identifiable by the sharp increase in amplitude and a phase change of  $\pi$  centered at this frequency. Despite the high excitation power, fits based on theoretical relations valid for small actuation force and amplitude<sup>33</sup> mostly show agreement with the experimental data. The amplitude is fitted to a Lorentzian equation and the phase to an inverse tangent relation. We extract mutually

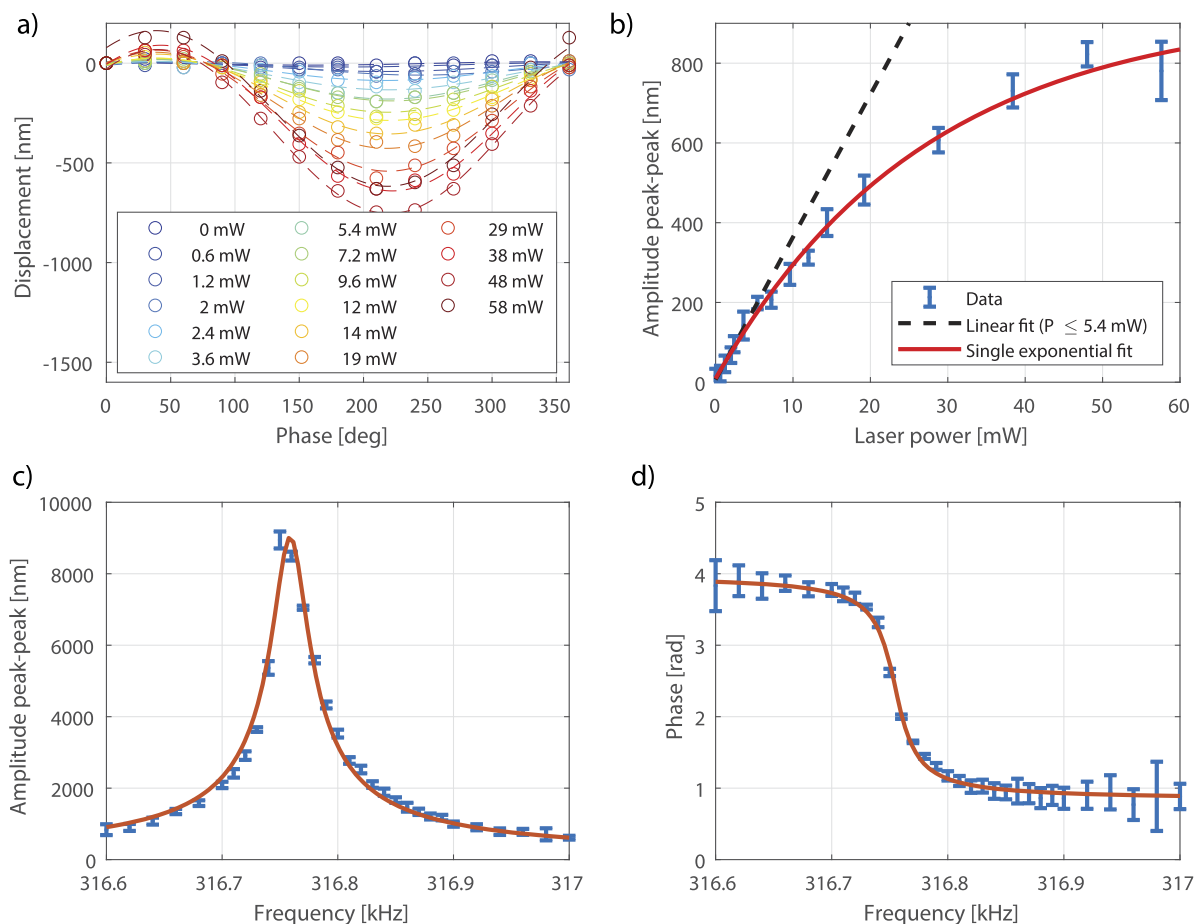


**FIG. 3.** Power and frequency dependency of cantilever oscillation as characterized with USEM. (a) Displacement derived from ultrafast movies for the indicated range of excitation powers at 317 kHz driving frequency. (b) The oscillation amplitude increases linearly with laser power in the low power regime, but it saturates according to a single exponential function for exciting powers on the order of tens of mW. (c) Varying the excitation frequency shows a clear resonance peak at 316.75 kHz and (d) corresponding shift of  $\pi$  for the phase between laser modulation and cantilever motion. The resonator has a Q-factor of  $1.1 \cdot 10^4$ .



corresponding Q-factors of  $1.03 \pm 0.15 \cdot 10^4$  and  $1.15 \pm 0.11 \cdot 10^4$  from fits to the amplitude and phase response, respectively. Furthermore, we notice the amplitude of the oscillation reaches a high peak value of  $9 \mu\text{m}$ , which brings imaging higher harmonic oscillations with reduced amplitude within reach.

Higher harmonic oscillations have a more complex mode shape as well as smaller amplitudes than the fundamental mode, adding to

the utility of large depth of focus real-space imaging combined with high resolution of the electron beam that USEM offers. We excite the second harmonic by focusing the laser on the middle of the cantilever for optimum excitation efficiency<sup>25,30</sup> with a power of 60 mW and a repetition frequency of 1.953 570 MHz and probe it with 20 ns electron pulses. An ultrafast movie of the oscillation was recorded and the dynamics visualized in Fig. 4 (multimedia

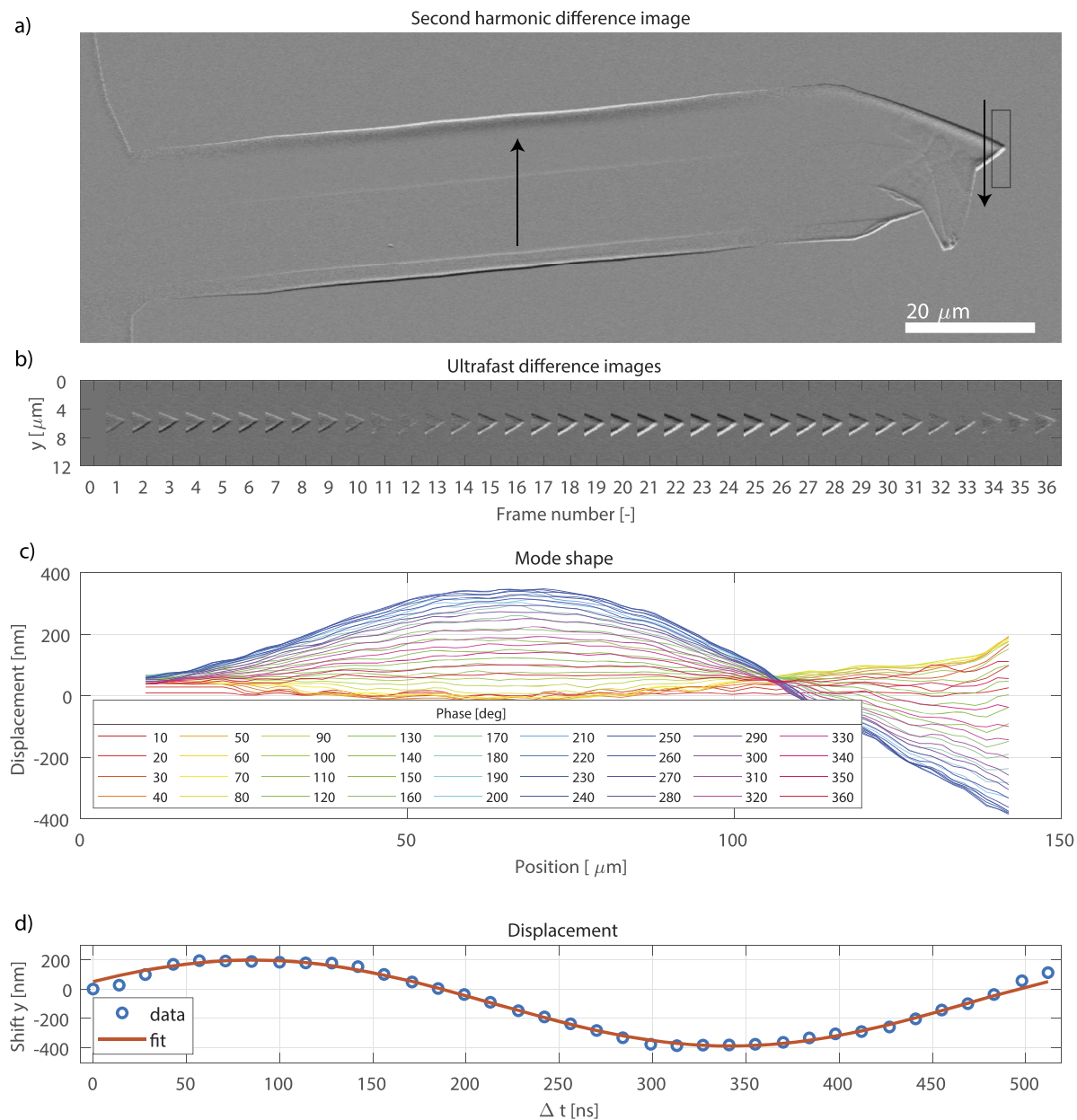


**FIG. 4.** The combination of high resolution and focus depth allows for tracking the mode shape of the second harmonic in time over the full length of the cantilever. (a) Difference image between  $230^\circ$  and  $50^\circ$  at second harmonic frequency showing movement in opposite direction at central part and tip of cantilever as indicated by the arrows. (b) Ultrafast difference images series of movement of cantilever tip [marked area in (a)]. (c) Plotting the displacement as a function of position for all phases highlights the characteristic shape of the second harmonic. (d) The tip displacement over time is sinusoidal in shape with 590 nm amplitude. Multimedia view: <https://doi.org/10.1063/5.0089086.2>

view). The movie is constructed of 37 frames with 14 ns time steps, equivalent to a 70 MHz sampling frequency; but with the 20 ns pulse duration, we effectively imaged at 50 MHz. This rate exceeds the 10 MHz detector bandwidth, and it can be further improved if required by simply reducing the electron pulse duration.

Both the movie and the difference images in Figs. 4(a) and 4(b) give qualitative insight into the mode shape, featuring displacement of the cantilever near the middle with the tip moving in opposite direction. The quantitative displacement over the full length of the cantilever, determined by comparing individual columns of pixels in the movie frames, is displayed in Fig. 4(c). Displacement down to the tens of nm scale is well defined over the full cantilever length. The curve shapes clearly represent the second harmonic with a node at around 75% of the cantilever length from the base and an amplitude of a few hundred nanometers at the antinodes. Displacement of the tip over time [Fig. 4(d)] shows sinusoidal motion with  $590 \pm 20$  nm peak–peak amplitude.

In conclusion, we have performed real-space time resolved imaging on a nanomechanical resonator at resonance, constructing ultrafast movies of a laser actuated cantilever with USEM. Large depth of focus allows for imaging the full cantilever in focus throughout the oscillation while the resolution is high enough to register displacement on the micro- and nanoscale. Moreover, the pulse duration can be selected to achieve high current to speed up acquisition or prioritize time resolution to image dynamics at rates beyond the detector bandwidth. Our work provides the prospect of real-space characterization and visualization of nanomechanical movement in MEMS resonators, aiding the development of new and bolstering our understanding of existing devices. Direct imaging of tip movement in close proximity to and interaction with a surface would be possible as is imaging nanomechanical cantilever mass sensors and other resonators exhibiting in-plane movement.

## SUPPLEMENTARY MATERIAL

See the [supplementary material](#) for an additional ultrafast video, measured with 100 ns electron pulse duration.

## ACKNOWLEDGMENTS

We thank Lodi Schriek for providing the AFM cantilevers.

## AUTHOR DECLARATIONS

### Conflict of Interest

The integrated light microscope served as a prototype for a product of Delmic B.V. in which P.K. and J.P.H. have a financial interest.

## Author Contributions

**Mathijs W.H. Garming:** Conceptualization (equal); Formal analysis (equal); Investigation (equal); Methodology (equal); Visualization (equal); Writing – original draft (equal); Writing – review & editing

(equal). **Pieter Kruit:** Conceptualization (equal); Funding acquisition (equal); Supervision (equal); Writing – review & editing (equal). **Jacob P. Hoogenboom:** Conceptualization (equal); Funding acquisition (equal); Supervision (equal); Writing – review & editing (equal).

## DATA AVAILABILITY

The data that support the findings of this study are available from the corresponding author upon reasonable request.

## REFERENCES

- 1 M. Henini, “Scanning electron microscopy: An introduction,” *III-Vs Review* **13**, 40–44 (2000).
- 2 A. H. Zewail, “Four-dimensional electron microscopy,” *Science* **328**, 187–193 (2010).
- 3 T. Liu, J. Y. Ou, E. Plum, K. F. MacDonald, and N. I. Zheludev, “Visualization of subatomic movements in nanostructures,” *Nano Lett.* **21**, 7746 (2021).
- 4 J. Spencer Baskin and A. H. Zewail, “Seeing in 4D with electrons: Development of ultrafast electron microscopy at Caltech,” *C. R. Phys.* **15**, 176–189 (2014).
- 5 A. Adhikari, J. K. Eliason, J. Sun, R. Bose, D. J. Flannigan, and O. F. Mohammed, “Four-dimensional ultrafast electron microscopy: Insights into an emerging technique,” *ACS Appl. Mater. Interfaces* **9**, 3–16 (2017).
- 6 M. W. H. Garming, M. Bolhuis, S. Conesa-Boj, P. Kruit, and J. P. Hoogenboom, “Lock-in ultrafast electron microscopy simultaneously visualizes carrier recombination and interface-mediated trapping,” *J. Phys. Chem. Lett.* **11**, 8880–8886 (2020).
- 7 M. W. H. Garming, I. G. C. Weppelman, M. Lee, T. Stavenga, and J. P. Hoogenboom, “Ultrafast scanning electron microscopy with sub-micrometer optical pump resolution,” *Appl. Phys. Rev.* **9**, 021418 (2022).
- 8 B. Arash, J.-W. Jiang, and T. Rabczuk, “A review on nanomechanical resonators and their applications in sensors and molecular transportation,” *Appl. Phys. Rev.* **2**, 021301 (2015).
- 9 R. Abdolvand, B. Bahreyni, J. Lee, and F. Nabki, “Micromachined resonators: A review,” *Micromachines* **7**, 160 (2016).
- 10 L. Wei, X. Kuai, Y. Bao, J. Wei, L. Yang, P. Song, M. Zhang, F. Yang, and X. Wang, “The recent progress of MEMS/NEMS resonators,” *Micromachines* **12**, 724 (2021).
- 11 G. Gruber, C. Urgell, A. Tavernarakis, A. Stavrinadis, S. Tepsic, C. Magén, S. Sangiao, J. M. De Teresa, P. Verlot, and A. Bachtold, “Mass sensing for the advanced fabrication of nanomechanical resonators,” *Nano Lett.* **19**, 6987–6992 (2019); [arXiv:2101.09201](#).
- 12 I. E. Rosłoń, R. J. Dolleman, H. Licon, M. Lee, M. Šiškins, H. Lebius, L. Madauf, M. Schleberger, F. Alijani, H. S. van der Zant, and P. G. Steeneken, “High-frequency gas effusion through nanopores in suspended graphene,” *Nat. Commun.* **11**, 6025 (2020).
- 13 M. Šiškins, M. Lee, S. Mañas-Valero, E. Coronado, Y. M. Blanter, H. S. van der Zant, and P. G. Steeneken, “Magnetic and electronic phase transitions probed by nanomechanical resonators,” *Nat. Commun.* **11**, 2698 (2020); [arXiv:1911.08537](#).
- 14 H. Hu, H. Cho, S. Somnath, A. F. Vakakis, and W. P. King, “Silicon nano-mechanical resonators fabricated by using tip-based nanofabrication,” *Nanotechnology* **25**, 275301 (2014).
- 15 H. Fujita, “Microactuators and micromachines,” *Proc. IEEE* **86**, 1721–1732 (1998).
- 16 B. Bhushan and O. Marti, “Scanning probe microscopy – Principle of operation, instrumentation, and probes,” in *Springer Handbook of Nanotechnology* (Springer, Berlin, Heidelberg, 2010), pp. 573–617.
- 17 L. Gross, B. Schuler, N. Pavliček, S. Fatayer, Z. Majzik, N. Moll, D. Peña, and G. Meyer, “Atomic force microscopy for molecular structure elucidation,” *Angew. Chem., Int. Ed.* **57**, 3888–3908 (2018).



- <sup>18</sup>A. Barg, Y. Tsaturyan, E. Belhage, W. H. P. Nielsen, C. B. Møller, and A. Schliesser, "Measuring and imaging nanomechanical motion with laser light," *Appl. Phys. B* **123**, 8 (2017).
- <sup>19</sup>S. J. Rothberg, M. S. Allen, P. Castellini, D. Di Maio, J. J. Dirckx, D. J. Ewins, B. J. Halkon, P. Muyschondt, N. Paone, T. Ryan, H. Steger, E. P. Tomasini, S. Vandanduit, and J. F. Vignola, "An international review of laser Doppler vibrometry: Making light work of vibration measurement," *Opt. Lasers Eng.* **99**, 11–22 (2017).
- <sup>20</sup>D. J. Flannigan, P. C. Samartzis, A. Yurtsever, and A. H. Zewail, "Nanomechanical motions of cantilevers: Direct imaging in real space and time with 4D electron microscopy," *Nano Lett.* **9**, 875–881 (2009).
- <sup>21</sup>N. Lobato-Dauzier, M. Denoual, T. Sato, S. Tachikawa, L. Jalabert, and H. Fujita, "Current driven magnetic actuation of a MEMS silicon beam in a transmission electron microscope," *Ultramicroscopy* **197**, 100–104 (2019).
- <sup>22</sup>Y. Zhang and D. J. Flannigan, "Observation of anisotropic strain-wave dynamics and few-layer dephasing in MoS<sub>2</sub> with ultrafast electron microscopy," *Nano Lett.* **19**, 8216–8224 (2019).
- <sup>23</sup>J. Hu, G. M. Vanacore, A. Cepellotti, N. Marzari, and A. H. Zewail, "Rippling ultrafast dynamics of suspended 2D monolayers, graphene," *Proc. Natl. Acad. Sci.* **113**, E6555–E6561 (2016).
- <sup>24</sup>R. J. Moerland, I. G. C. Weppelman, M. W. H. Garming, P. Kruit, and J. P. Hoogenboom, "Time-resolved cathodoluminescence microscopy with sub-nanosecond beam blanking for direct evaluation of the local density of states," *Opt. Express* **24**, 24760 (2016).
- <sup>25</sup>M. Vassalli, V. Pini, and B. Tiribilli, "Role of the driving laser position on atomic force microscopy cantilevers excited by photothermal and radiation pressure effects," *Appl. Phys. Lett.* **97**, 143105 (2010).
- <sup>26</sup>D. Kiracofe, K. Kobayashi, A. Labuda, A. Raman, and H. Yamada, "High efficiency laser photothermal excitation of microcantilever vibrations in air and liquids," *Rev. Sci. Instrum.* **82**, 013702 (2011).
- <sup>27</sup>M. Guizar-Sicairos, S. T. Thurman, and J. R. Fienup, "Efficient subpixel image registration algorithms," *Opt. Lett.* **33**, 156 (2008).
- <sup>28</sup>C. Van Der Avoort, R. Van Der Hout, J. J. Bontemps, P. G. Steeneken, K. Le Phan, R. H. Fey, J. Hulshof, and J. T. Van Beek, "Amplitude saturation of MEMS resonators explained by autoparametric resonance," *J. Micromech. Microeng.* **20**, 105012 (2010).
- <sup>29</sup>J. Jahng, D. A. Fishman, S. Park, D. B. Nowak, W. A. Morrison, H. K. Wickramasinghe, and E. O. Potma, "Linear and nonlinear optical spectroscopy at the nanoscale with photoinduced force microscopy," *Acc. Chem. Res.* **48**, 2671–2679 (2015).
- <sup>30</sup>B. A. Bircher, L. Duempelmann, H. P. Lang, C. Gerber, and T. Braun, "Photothermal excitation of microcantilevers in liquid: Effect of the excitation laser position on temperature and vibrational amplitude," *Micro Nano Lett.* **8**, 770–774 (2013).
- <sup>31</sup>G. Gruca, D. Chavan, J. Rector, K. Heeck, and D. Iannuzzi, "Demonstration of an optically actuated ferrule-top device for pressure and humidity sensing," *Sens. Actuators, A* **190**, 77–83 (2013).
- <sup>32</sup>Y. Miyahara, H. Griffin, A. Roy-Gobeil, R. Belyansky, H. Bergeron, J. Bustamante, and P. Grutter, "Optical excitation of atomic force microscopy cantilever for accurate spectroscopic measurements," *EPJ Tech. Instrum.* **7**, 2 (2020); [arXiv:1910.11895](https://arxiv.org/abs/1910.11895).
- <sup>33</sup>H. J. R. Westra, *Nonlinear Beam Mechanics* (Delft University of Technology, 2012), p. 16.